

# 1 N-Heterocyclic Carbenes: A Door Open to Supramolecular 2 Organometallic Chemistry

3 Susana Ibáñez, Macarena Poyatos, and Eduardo Peris\*



Cite This: <https://dx.doi.org/10.1021/acs.accounts.0c00312>



Read Online

ACCESS |



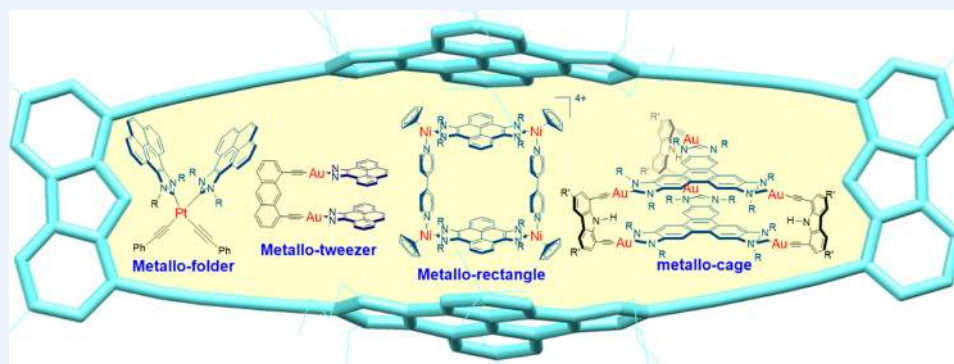
Metrics & More



Article Recommendations



Supporting Information



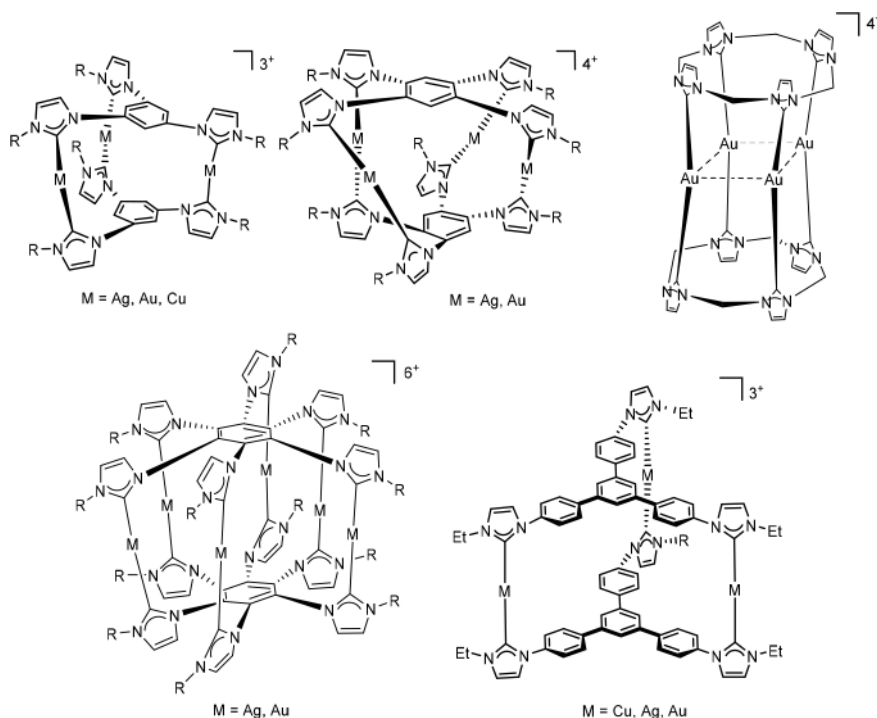
4 **CONSPECTUS:** The field of metallosupramolecular chemistry is clearly dominated by the use of O-, N-, and P-donor Werner-type  
5 polydentate ligands. These molecular architectures are of high interest because of their wide range of applications, which include  
6 molecular encapsulation, stabilization of reactive species, supramolecular catalysis, and drug delivery, among others. Only recently,  
7 organometallic ligands have allowed the preparation of a variety of supramolecular coordination complexes, and the term  
8 supramolecular organometallic complexes (SOCs) is gaining space within the field of metallosupramolecular chemistry. While the  
9 early examples of SOC s referred to supramolecular architectures mostly containing bisalkenyl, diphenyl, or bisalkynyl linkers, the  
10 development of SOC s during the past decade has been boosted by the parallel development of multidentate N-heterocyclic carbene  
11 (NHC) ligands. The first examples of NHC-based SOC s referred to supramolecular assemblies based on polydentate NHC ligands  
12 bound to group 11 metals. However, during the last 10 years, several planar poly-NHC ligands containing extended  $\pi$ -conjugated  
13 systems have facilitated the formation of a large variety of architectures in which the supramolecular assemblies can contain metals  
14 other than Cu, Ag, and Au. Such ligands are Janus di-NHCs and trigonal-planar tris-NHCs—most of them prepared by our research  
15 group—which have allowed the preparation of a vast range of NHC-based metallosupramolecular compounds with interesting host–  
16 guest chemistry properties. Although the number of SOC s has increased in the past few years, their use for host–guest chemistry  
17 purposes is still in its earliest infancy. In this Account, we describe the achievements that we have made during the last 4 years  
18 toward broadening the applications of planar extended  $\pi$ -conjugated NHC ligands for the preparation of organometallic-based  
19 supramolecular structures, including their use as hosts for some selected organic and inorganic guests, together with the catalytic  
20 properties displayed by some selected host–guest inclusion complexes. Our contribution describes the design of several Ni-, Pd-, and  
21 Au-based metallorectangles and metalloprisms, which we used for the encapsulation of several organic substrates, such as polycyclic  
22 aromatic hydrocarbons (PAHs) and fullerenes. The large binding affinities found are ascribed to the incorporation of two cofacial  
23 panels with large  $\pi$ -conjugated systems, which provide the optimum conditions for guest recognition by  $\pi$ – $\pi$ -stacking interactions.  
24 We also describe a series of digold(I) metallotweezers for the recognition of organic and inorganic substrates. These metallotweezers  
25 were used for the recognition of “naked” metal cations and polycyclic aromatic hydrocarbons. The recognition properties of these  
26 metallotweezers are highly dependent on the nature of the rigid connector and of the ancillary ligands that constitute the arms of the  
27 tweezer. A peculiar balance between the self-aggregation properties of the tweezer and its ability to encapsulate organic guests is  
28 observed.

## 1. INTRODUCTION

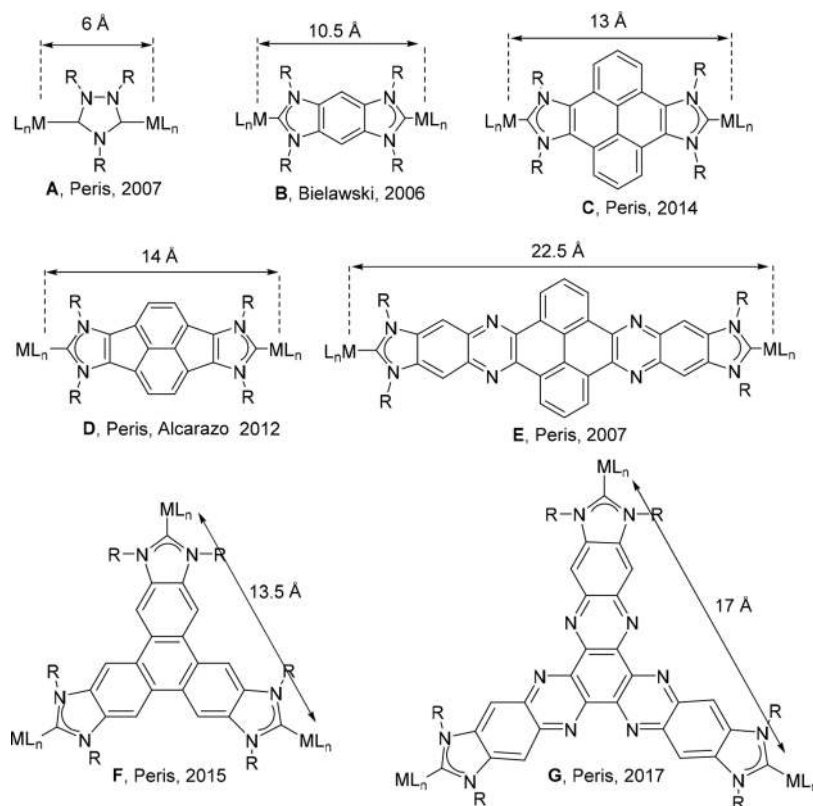
29 Metallosupramolecular chemistry refers to the field of research  
30 involving the combination of bridging organic ligands with metal  
31 units that form discrete or polymeric assemblies of different  
32 shapes and sizes.<sup>1</sup> Over the last three decades, coordination-  
33 driven self-assembly has become a widespread strategy for the

Received: May 22, 2020

Scheme 1. Some NHC-Based SOCs with Group 11 Metals



Scheme 2. Planar Di- and Tri-NHC Ligands for the Preparation of SOCs



34 rational construction of discrete supramolecular coordination  
 35 complexes (SCCs).<sup>1a,2</sup> This technique capitalizes on the  
 36 directional and predictable nature of the metal–ligand bond,  
 37 which allows the outcome of the self-assembly process to be  
 38 predicted with a high level of certainty. Many of the reported  
 39 SCCs have discrete void areas with well-defined shapes and

sizes, and this is why SCCs are often called “molecular flasks”.<sup>3</sup>  
 40 These cavities impart unique properties to the structure that lead  
 41 to novel functions and applications. For the design of these void  
 42 spaces, the ligand is arguably the most important building block  
 43 because its topological features and binding abilities determine  
 44 the size, geometry, and functionality of the resulting cavities. 45

46 From the ligand perspective, metallosupramolecular chemistry  
47 is clearly dominated by the use of O-, N-, and P-donor Werner-  
48 type polydentate ligands, while only a few examples of  
49 assemblies bearing carbon donor ligands have been reported  
50 in the literature. However, during the past decade, the number of  
51 organometallic-based supramolecular assemblies has grown fast  
52 and parallel to the development of multidentate N-heterocyclic  
53 carbene (NHC) ligands,<sup>4</sup> and a number of review articles were  
54 published recently.<sup>5</sup> The rapid development of supramolecular  
55 assemblies with organometallic ligands is exemplified by the  
56 establishment of the term supramolecular organometallic  
57 complexes (SOCs), coined by Pöthig and Casini in 2019,<sup>5c</sup> to  
58 refer to complexes in which the (organic) linker forms the  
59 organometallic bond to the metal node. This means that the  
60 carbon–metal bond is structurally crucial for the formation of  
61 the architecture of the resulting SOC, in contrast to those  
62 assemblies that do not have organometallic-based ligands or  
63 those whose organometallic ligands (normally  $\eta^5$ -Cp or  $\eta^6$ -  
64 arene) cap the metal nodes.

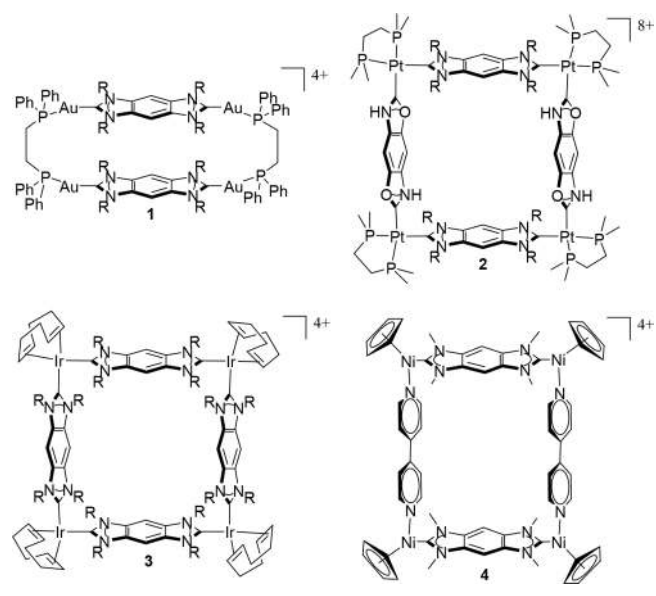
65 Most NHC-based SOC are supramolecular assemblies based  
66 on polydentate NHC ligands bound to group 11 metals. The  
67 reason for this is that these metals often display linear  
68 coordination modes that facilitate trans coordination of the  
69 NHC ligands, thereby forming assemblies in which the metal  
70 atoms are sandwiched between the two polydentate NHC  
71 ligands. In addition, the NHC–M bond (M = Cu, Ag, Au) is  
72 usually labile, which allows the formation of the thermodynami-  
73 cally most stable assemblies from mixtures of the metal  
74 precursors and the poly-NHC. These assemblies include  
75 rectangles, triangles,<sup>6</sup> and cylinders,<sup>7</sup> such as the ones shown  
76 in Scheme 1.

77 However, during the last 10 years, several planar poly-  
78 conjugated poly-NHC ligands have facilitated the formation of a  
79 variety of structures in which the supramolecular assemblies can  
80 contain metals other than Cu, Ag, and Au.<sup>8</sup> The use of the Janus  
81 di-NHC ligands A–E (Scheme 2) allows the synthesis of  
82 supramolecular assemblies whose dimensions may range from 6  
83 Å as established by triazolylidene ligand A<sup>8a</sup> to almost 23 Å when  
84 the nanosized di-NHC with the quinoxalinophenanthrophen-  
85 azine core E<sup>8e</sup> is used. Among these, the benzobis-  
86 (imidazolylidene) ligand B described by Bielawski in 2005<sup>9</sup>  
87 was the first one to demonstrate its suitability for the preparation  
88 of organometallic-based assemblies. Some threefold-symmetric  
89 tri-NHCs, such as F and G, have also been prepared.<sup>8d,f,10</sup>

90 Hahn's group was the first one to exploit the linear  
91 arrangement of B for the preparation of a number of square-  
92 and rectangular-shaped assemblies that included metals such as  
93 gold,<sup>11</sup> iridium,<sup>12</sup> platinum,<sup>13</sup> palladium,<sup>12b</sup> and nickel<sup>14</sup>  
94 (Scheme 3). Together with the use of this benzobis-  
95 (imidazolylidene) ligand, Hahn also used a structurally similar  
96 di(NH,O)-NHC ligand for the preparation of a large number of  
97 molecular squares.<sup>6a,b</sup> The benzobis(NHC) ligand B establishes  
98 a metal-to-metal separation of 10.5 Å, which in most cases is too  
99 small to build cavities of the appropriate size to host organic  
100 guests. This is probably the reason why none of the  
101 organometallic assemblies displayed in Scheme 3 were used  
102 for host–guest chemistry purposes.

103 Although the number of SOC has increased in the past few  
104 years, those used for host–guest chemistry purposes are still very  
105 few. Some recent relevant examples of SOC used for the  
106 encapsulation of organic substrates were described by Altmann  
107 and Pöthig,<sup>15</sup> who developed organometallic-based rotaxanes  
108 consisting of Ag<sub>8</sub> and Au<sub>8</sub> pillarplexes, which are highly selective

### Scheme 3. NHC-Based Metallosquares Described by Hahn's Group



109 for the encapsulation of linear molecules, such as 1,8-  
110 diaminoctane. These metallosupramolecules also showed  
111 important antimicrobial activity and anticancer properties.<sup>16</sup>

112 With all of these precedents in hand, 4 years ago we started a  
113 new research line aiming to provide effective synthetic routes to  
114 NHC-based SOC with applications in catalysis and host–guest  
115 chemistry. A clear advantage for us is that during the past few  
116 years we have prepared a large number of planar di- and tri-NHC  
117 ligands bearing  $\pi$ -extended polyconjugated cores such as those  
118 shown in Scheme 2, so we thought that this placed us in a  
119 privileged position to approach this new research line. In  
120 addition, our previous studies on the influence of supra-  
121 molecular interactions on homogeneously catalyzed reactions<sup>17</sup>  
122 had already constituted our initial approach to metallosupra-  
123 molecular chemistry and thus gave us some expertise in the field.  
124 This Account focuses on our achievements in the development  
125 of NHC-based SOC that we prepared during the last 4 years,  
126 emphasizing their use as hosts for some selected organic and  
127 inorganic guests. The Account thus covers our progress in the  
128 development of several Ni-, Pd-, and Au-based metallorectan-  
129 gles, metalloprisms, and metaltweezers together with their  
130 respective host–guest chemistry properties.

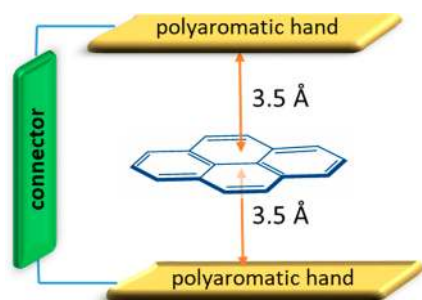
## 2. STRUCTURES WITH MONO-NHC LIGANDS: METALLOFOLDERS AND METALLOTWEEZERS

131 A molecular tweezer is a molecular receptor that contains two  
132 identical flat polyaromatic arms at the edges that are connected  
133 in a syn conformation by a more-or-less rigid tether (Scheme  
134 4).<sup>18</sup> In order to enable complexation with aromatic substrates  
135 s4 by  $\pi$ – $\pi$ -stacking interactions, the two parallel polyaromatic  
136 hands should be ideally separated by  $\sim 7$  Å, as aromatic groups  
137 stack at an interplanar distance of  $\leq 3.5$  Å.  
138

139 While molecular tweezers were initially based on organic  
140 entities, in the past decade some research groups have  
141 incorporated metals into the structure of the tweezers, thus  
142 introducing a new dimension into the properties of these  
143 supramolecular systems.<sup>19</sup> Our first approach to the develop-  
144 ment of metaltweezers was the preparation of a series of Pt(II)  
145 s5 complexes bearing cis-oriented NHC ligands decorated with  $\pi$ -



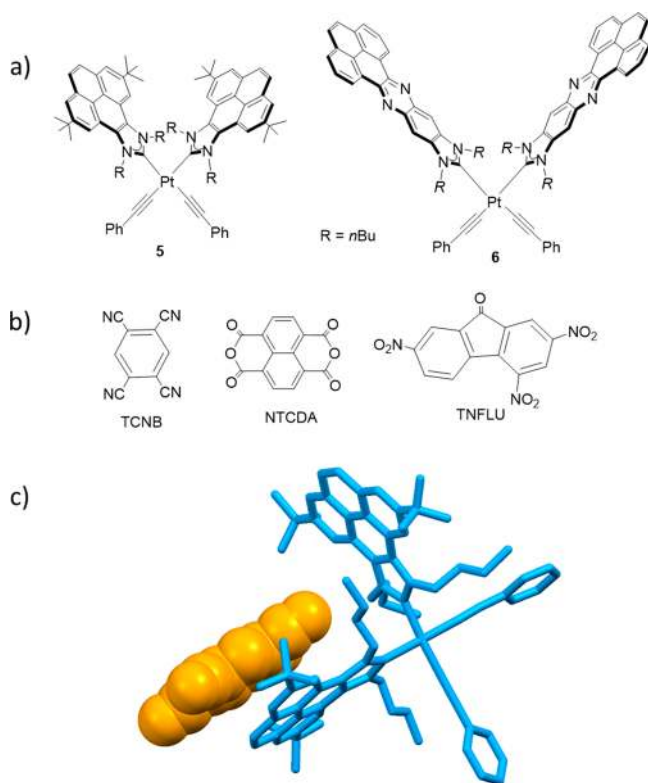
#### Scheme 4. Schematic Representation of a Molecular Tweezer Trapping a Molecule of Pyrene



these two receptors are due to the orthogonal disposition of the two polyaromatic panels, which prevents their cooperative  $\pi$ - $\pi$ -stacking interaction with the guests, as would have probably happened if the two panels were disposed in a parallel manner.

Our next approach for the preparation of metallotweezers was the synthesis of complex **7** (Scheme 6), which contains two Au(I) pyrene-imidazolylidene arms connected by a 1,8-diethynylantracene linker.<sup>21</sup> In principle, this metallotweezer should show interesting recognition abilities since the two polyaromatic panels are parallel and separated by approximately 7 Å. However, the supramolecular properties of **7** are markedly determined by its tendency to self-aggregate. In a nonpolar solvent such as benzene, **7** self-aggregates to form the duplex complex (**7**)<sub>2</sub> (Scheme 6). This self-complementary duplex complex is formed by the encapsulation of the anthracenyl linker of each tweezer between the two pyrene-functionalized arms of the complementary one. The molecular structure of the complex shows that the four gold atoms form a rectangle displaying strong auophobic interactions between the pairs of gold atoms of complementary tweezers. In the presence of “naked” metal cations (Cu<sup>+</sup>, Ag<sup>+</sup>, or Tl<sup>+</sup>), the tweezer is able to self-aggregate in CH<sub>2</sub>Cl<sub>2</sub>, thus forming a similar duplex complex in which the metal cation is trapped inside the small cavity formed by the supramolecular assembly, as shown in Scheme 5 for the case of the addition of Ag<sup>+</sup>. The self-aggregated structures formed are stabilized by a combination of  $\pi$ - $\pi$ -stacking and M–Au metallophilic interactions. Titrations by fluorescence spectroscopy allowed the determination of the large association constants of the resulting inclusion duplex complexes formed by addition of the metal cations.

#### Scheme 5. (a) Platinum-Based Metallofolders **5** and **6**; (b) Guests Used in the Study; (c) Molecular Structure of TCNB@**5**

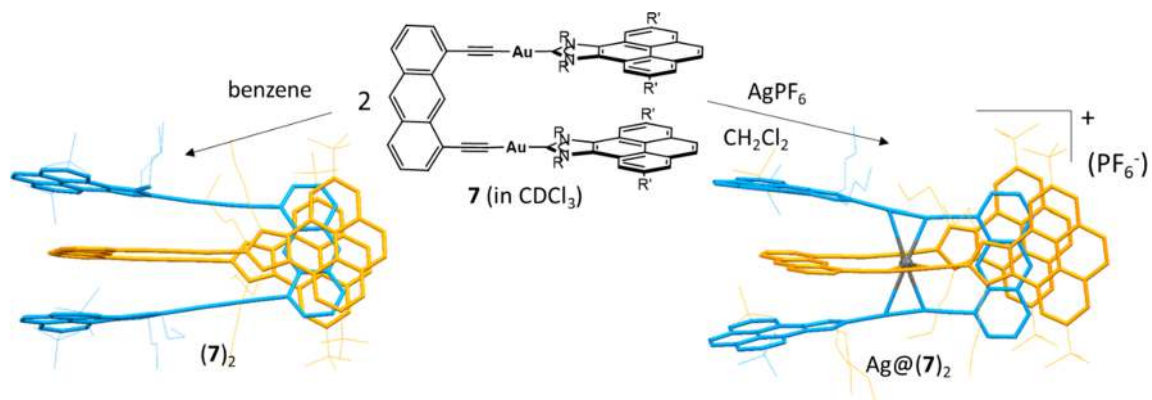
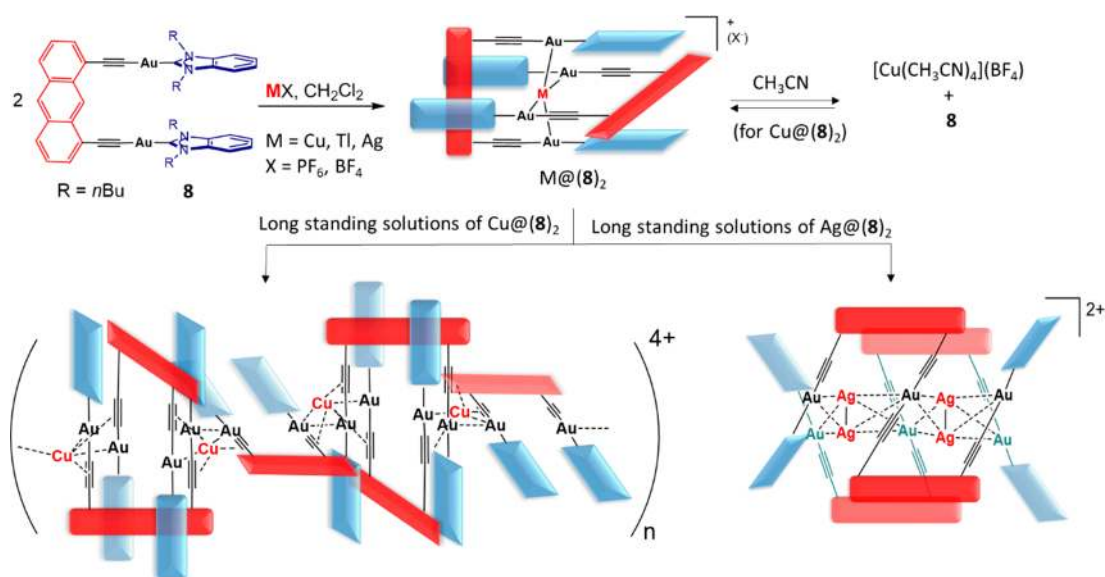
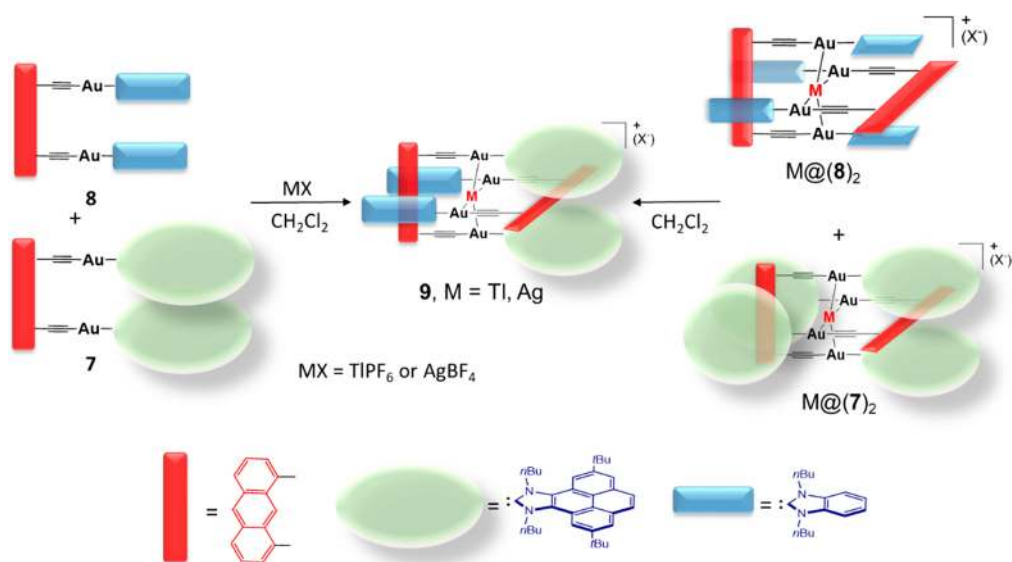


We were interested in studying how subtle modifications of the structure of **7** would affect the supramolecular properties of the resulting complex. We first obtained the new metallotweezer **8** (Scheme 7) in which we changed the pyrene-imidazolylidene ligand to a smaller benzoimidazolylidene. It was anticipated that this would reduce the ability of the complex to self-aggregate because the  $\pi$ -delocalized surface area of the ligand is smaller than that shown by the pyrene-functionalized ligand in **7**. In fact, we observed that in the absence of an external stimulus, **8** does not show any tendency to self-aggregate. However, the addition of Cu<sup>+</sup>, Tl<sup>+</sup>, or Ag<sup>+</sup> facilitated the formation of self-aggregated structures in which the metal cations occupied the cavity of the dimer, although the three different species showed very distinctive behaviors. The complex with copper showed an interesting naked-eye-perceivable color change response (orange to yellow) to the presence of acetonitrile or ammonia vapors. This color change reverts after a few minutes upon exposure to air, and the process is fully reversible, as demonstrated through numerous cycles. This reversible vapo-chromism is explained by the formation of [Cu(CH<sub>3</sub>CN)<sub>4</sub>](BF<sub>4</sub>) or [Cu(NH<sub>3</sub>)<sub>4</sub>](BF<sub>4</sub>) upon exposure of Cu@(**8**)<sub>2</sub> to vapors of acetonitrile and ammonia, respectively, with the concomitant formation of **8**. In addition, while solutions of the thallium-trapped species Tl@(**8**)<sub>2</sub> were stable for days, the compounds containing copper and silver evolved into a polymer (Cu) or an oligomer (Ag) (Scheme 7). The different reactivity patterns shown by **8** and the pyrene-containing tweezer **7** are explained because  $\pi$ - $\pi$ -stacking interactions are less likely to be produced in **8**, and therefore, the molecule may self-aggregate, but the process is reversible and may also give rise to more complex structures such as oligomers and polymers.

Once we studied the self-aggregation properties of tweezers **7** and **8**, we became interested in studying the cation-triggered

extended polyaromatic moieties (Scheme 5a).<sup>20</sup> The orthogonal disposition of the two aromatic hands of the receptor made us

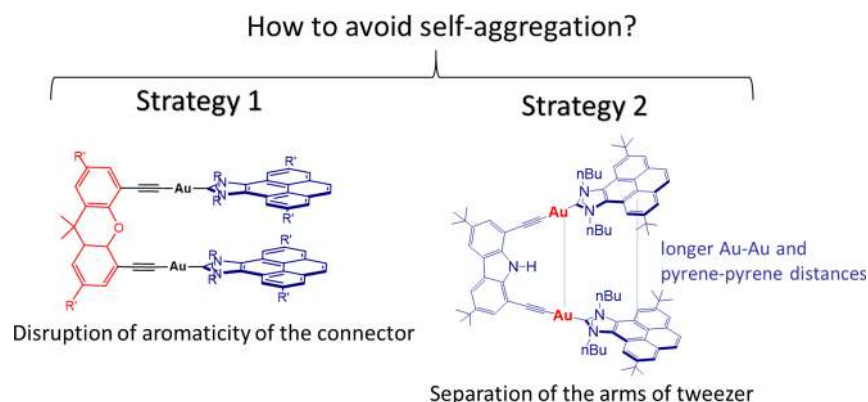
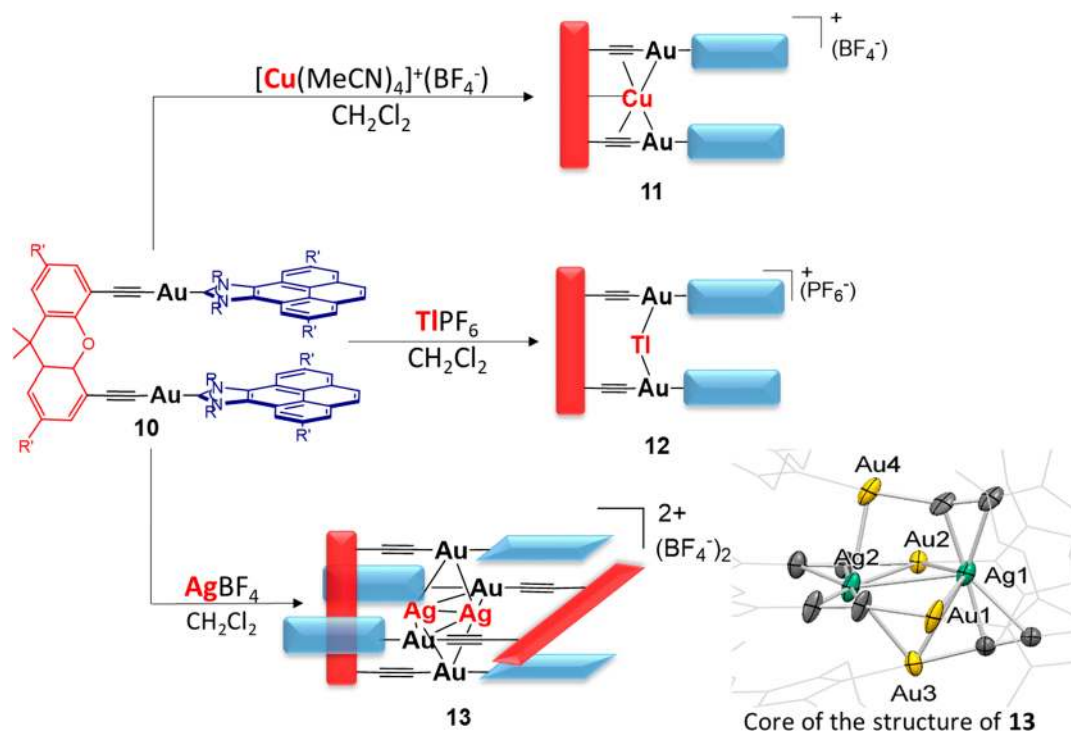
consider that the term *metallofolders* would be more accurate to refer to this subclass of metallotweezers. By taking advantage of the void space between the polyaromatic panels, these complexes were used as receptors of electron-deficient organic molecules such as 1,2,4,5-tetracyanobenzene (TCNB), 2,4,7-trinitro-9-fluorenone (TNFLU), and 1,4,5,8-naphthalenetetracarboxylic dianhydride (NTCDA). Although the host-guest association constants were low, we observed that the receptors were able to discriminate between electron-rich and electron-deficient aromatic substrates. Besides, we observed that molecule **6** containing the phenanthrophenazine panel was a more effective receptor than molecule **5** containing pyrene, most likely because of the larger surface area provided by the former one, which renders a more effective  $\pi$ - $\pi$ -stacking interaction with the guests.<sup>20</sup> The relatively low binding affinities shown by

Scheme 6. Self-Aggregation of **7** in Benzene and in the Presence of  $\text{Ag}^+$ Scheme 7. Reactivity Shown by **8** upon Addition of  $\text{Cu}^+$ ,  $\text{Tl}^+$ , or  $\text{Ag}^+$ Scheme 8. Social Self-Sorting Involving Mixtures of Complexes **7** and **8**

226 self-association properties of mixtures of these two different  
227 metallotweezers in order to determine whether any selectivity

was produced in the formation of the resulting molecular 228  
aggregates.<sup>23</sup> As depicted in Scheme 8, the reactions of 229 s8

## Scheme 9. Strategies for Avoiding the Self-Aggregation of Au(I) Metallotweezers

Scheme 10. Distinct Coordination Modes of 10 with Cu<sup>+</sup>, Tl<sup>+</sup>, and Ag<sup>+</sup>

230 equimolar mixtures of 7 and 8 with TlPF<sub>6</sub> or AgBF<sub>4</sub> exclusively  
 231 yielded the heterocomplexes 9, in which the two different  
 232 metallotweezers with the two different NHC-based ligands  
 233 aggregate, indicating that for this process the product was  
 234 obtained through a highly selective social self-sorting event. The  
 235 reactions between the homocomplex dimers containing thallium  
 236 or silver also evolved to the related mixed-ligand hetero-  
 237 complexes 9, thus indicating that 9 is the thermodynamically  
 238 (rather than kinetically) favored species. The formation of 9 was  
 239 assumed to be a consequence of the maximization of the  $\pi$ - $\pi$ -  
 240 stacking and metallophilic interactions in the aggregated  
 241 structures.<sup>23</sup> Other examples of self-sorting phenomena shown  
 242 by NHC-based assemblies have been reported recently.<sup>6c,24</sup>

243 As can be seen from the description of the properties of 7 and  
 244 8, it became evident that their supramolecular properties are  
 245 determined by their tendency to self-aggregate. In order to use a  
 246 metallotweezer for the recognition of aromatic substrates, we  
 247 needed to minimize the self-aggregation tendency so that the  
 248 two polyaromatic arms of the receptor would be exclusively used

to trap a potential aromatic guest. In order to reduce the self-  
 complementary character of the tweezers, we thought of two  
 different strategies. The first involved designing a new  
 metallotweezer with a linker in which the  $\pi$ -extended system is  
 disrupted, so that its participation in the  $\pi$ - $\pi$ -stacking event is  
 less likely to occur (Scheme 9, strategy 1). The second strategy  
 consists of using a linker with two diverging alkyne ligands, so  
 that the two polyaromatic arms of the tweezer are separated by  
 a distance that prevents their participation in the self-aggregation  
 process (Scheme 9, strategy 2).

To implement the first strategy, we prepared U-shaped digold  
 metallotweezer 10 with a bis(alkynyl)xanthene connector  
 (Scheme 10).<sup>25</sup> This metallotweezer acts as metalloligand in  
 the presence of Cu<sup>+</sup>, Tl<sup>+</sup>, or Ag<sup>+</sup>, and we observed that the  
 coordination ability of the metalloligand was highly dependent  
 on the cation used. All of the coordination modes are highly  
 influenced by strong M...Au interactions. Coordination to Cu<sup>+</sup>  
 leads to a complex in which the metalloligand is coordinated in a  
 pincer form (11), with the copper atom bound to the two



268 alkynyls and to the oxygen of the xanthene linker. In addition,  
 269 the copper(I) atom is also a very short distance from the Au  
 270 atoms, indicating strong metallophilic interactions. The reaction  
 271 of **10** with  $\text{Tl}^+$  affords a complex in which the ligand acts as a  
 272 *trans*- $\kappa^2$  chelate ligand through two  $\text{Tl}$ -Au metallophilic  
 273 interactions (**12**). The reaction with  $\text{Ag}^+$  leads to a self-  
 274 assembled structure with two silver cations encased inside the  
 275 cavity of a duplex structure formed by two self-assembled  
 276 metallotweezers (**13**). The reason for the formation of this  
 277 structure is found in the core of the molecule, in which it can be  
 278 observed that the two silver atoms maximize all possible  
 279 interactions with the binding sites of the metalloligand (alkynyls  
 280 and gold atoms) with additional stabilization by the formation of  
 281 a Ag-Ag argentophilic bond (Scheme 10).<sup>25</sup>

282 The second strategy that we used to avoid the self-association  
 283 of the metallotweezers was to use a linker with two diverging  
 284 alkynyl groups. Complex **14** contains a bis(alkynyl)carbazole  
 285 connector with two pyrene-imidazolylidene-Au(I) arms. As  
 286 can be observed from the molecular structure of the complex  
 287 (Figure 1a), the two pyrene moieties are separated by a distance

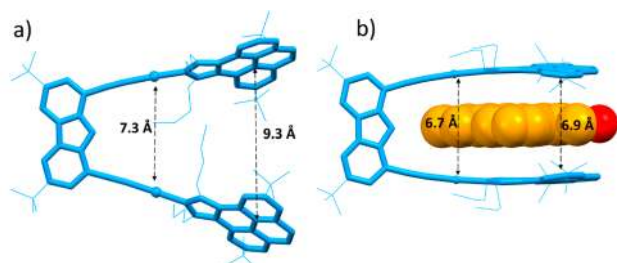


**Figure 1.** Molecular structures of (a) **14** and (b) 3-perylenylmethanol@**14** (oxygen atom of guest in red).

288 of 9.3 Å, which is too large to facilitate the self-aggregation of the  
 289 complex.<sup>26</sup> However, the two arms are flexible enough to reduce  
 290 this distance to 6.9 Å so that the two pyrene arms can approach  
 291 the surface of a polyaromatic guest such as 3-perylenylmethanol  
 292 (Figure 1b), facilitating maximum face-to-face overlap.

293 Complex **14** was used for the recognition of a series of  
 294 polycyclic aromatic hydrocarbons (PAHs). The compound is  
 295 able to bind these planar polyaromatic guests as a result of the  
 296  $\pi$ - $\pi$ -stacking interactions between the polyaromatic guests and  
 297 the pyrene moieties of the NHC ligand.<sup>26</sup> In addition, the  
 298 presence of the NH group in the carbazole tether strengthens the  
 299 binding of those PAHs functionalized with groups capable of  
 300 hydrogen bonding, as concluded from our experimental and  
 301 density functional theory (DFT) studies. The association  
 302 constants of these guests are up to 1 order of magnitude larger  
 303 than those shown by unfunctionalized PAHs. For example, the  
 304 association constant between **14** and pyrene is  $10 \text{ M}^{-1}$  in

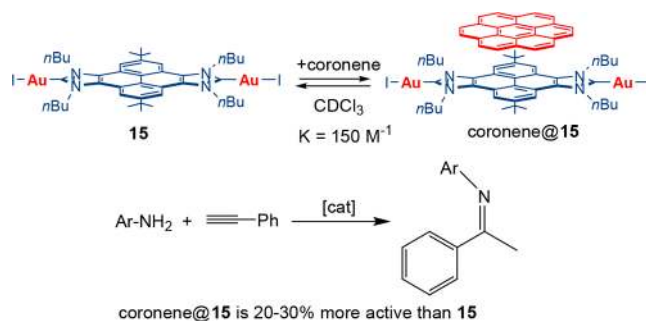
toluene, while the constant with 1-pyrenylmethanol is  $340 \text{ M}^{-1}$ ,<sup>305</sup>  
 as shown in Scheme 11. Similarly, the association constant of **14**<sup>306 s12</sup>  
 with perylene is  $145 \text{ M}^{-1}$ , while the constant with 3-<sup>307</sup>  
 perylenylmethanol is  $1350 \text{ M}^{-1}$ .<sup>26</sup> These findings demonstrate<sup>308</sup>  
 that the combination of  $\pi$ - $\pi$ -stacking and hydrogen-bonding<sup>309</sup>  
 interactions can be used for the rational design of more efficient<sup>310</sup>  
 metalloceptors.<sup>311</sup>

### 3. STRUCTURES WITH DI- AND TRI-NHC LIGANDS

#### 3.1. Dimetallic Structures with Janus Di-NHCs

In 2018 we studied the binding affinities of **15**, a digold(I)<sup>312</sup>  
 complex with a pyrenebis(imidazolylidene) ligand (Scheme 12),<sup>313 s12</sup>

**Scheme 12.** Binding of **15** with Coronene and Effect on Catalysis



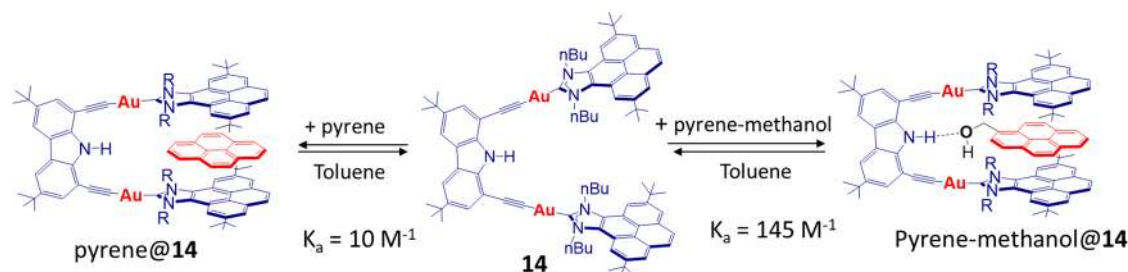
with a series of polycyclic aromatic hydrocarbons.<sup>27</sup> The<sup>314</sup>  
 presence of the pyrene moiety in the complex serves as a  $\pi$ - $\pi$ -<sup>315</sup>  
 stacking platform for binding of PAHs, and an association<sup>316</sup>  
 constant of  $150 \text{ M}^{-1}$  was determined for the binding of **15** with<sup>317</sup>  
 coronene in chloroform. Interestingly, the catalytic activity of<sup>318</sup>  
 the complex toward the hydroamination of phenylacetylene<sup>319</sup>  
 with primary amines was improved by 20–30% upon the<sup>320</sup>  
 addition of coronene to the reaction medium. The study<sup>321</sup>  
 demonstrated how the activity of a homogeneous catalyst can be<sup>322</sup>  
 highly influenced by supramolecular interactions with an<sup>323</sup>  
 external additive.<sup>27</sup><sup>324</sup>

We also prepared a di-NHC ligand connected by a<sup>325</sup>  
 corannulene moiety that we coordinated to gold to afford<sup>326</sup>  
 complex **16** (Scheme 13). We took advantage of the bowl-<sup>327 s13</sup>  
 shaped nature of corannulene to use complex **16** as a receptor for<sup>328</sup>  
 the recognition of fullerene  $\text{C}_{60}$ . Because of the excellent shape<sup>329</sup>  
 complementarity, **16** and  $\text{C}_{60}$  showed an excellent binding<sup>330</sup>  
 affinity in toluene solution, producing guest:host complexes<sup>331</sup>  
 with stoichiometries of up to 1:3, as depicted in Scheme 13.<sup>332</sup>

#### 3.2. Au-Based Metallorectangles and Metallocages

The two examples shown in Schemes 12 and 13 constitute good<sup>333</sup>  
 illustrations of how the introduction of extended  $\pi$ -conjugated<sup>334</sup>

**Scheme 11.** Binding of **14** with Pyrene and 1-Pyrenylmethanol



**Scheme 13. Reaction of 16 with C<sub>60</sub>; The DFT-Calculated Structure of the Product Is Shown**

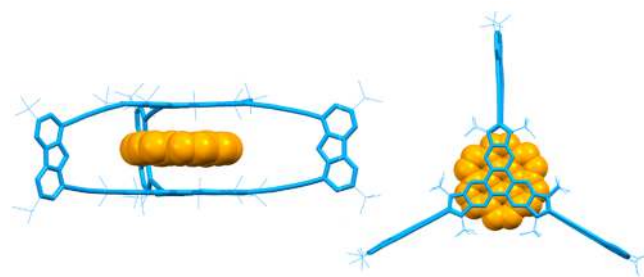
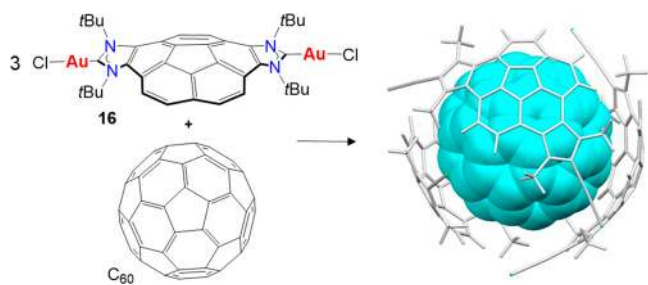


**Figure 2.** Two perspectives of the molecular structure of coronene@18.

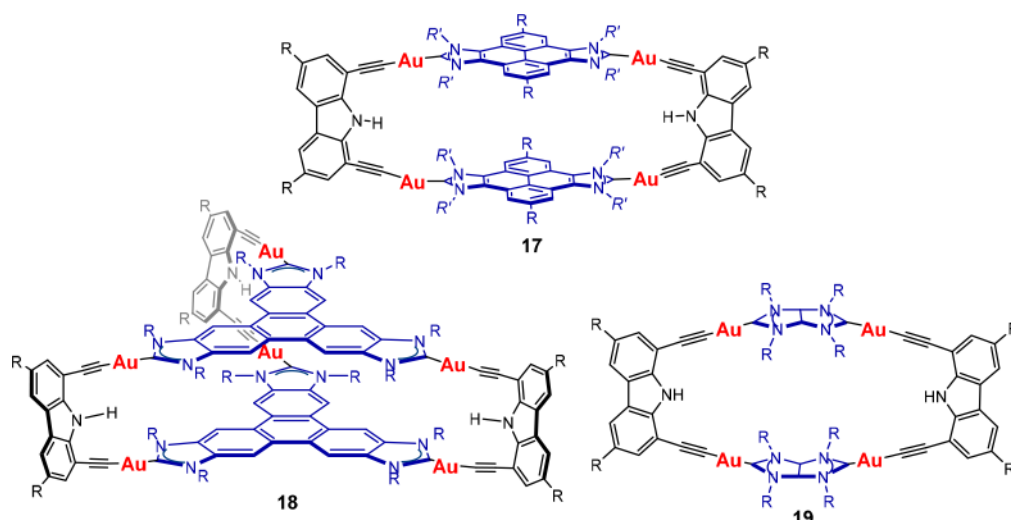
s14  
f2

335 systems into the structure of Janus-type di-NHC ligands can  
336 bring interesting properties into the resulting complexes due to  
337 the establishment of  $\pi$ - $\pi$ -stacking interactions with polyar-  
338 omatic guests. The results are even more interesting if we  
339 consider that the two examples shown before refer to complexes  
340 with open structures lacking well-defined closed cavities. With  
341 these results in hand, we thought that the introduction of this  
342 type of ligand into the structure of closed metallocages should  
343 produce metallosupramolecular assemblies with enhanced  
344 host-guest chemistry abilities. Given our previous results on  
345 the preparation of gold-based metallotweezers, we aimed to  
346 obtain a set of new metallocages by replacing the mono-NHC  
347 ligands by di- and tri-NHC ligands connected by extended  $\pi$ -  
348 conjugated systems. Using this strategy and the bis(alkynyl)-  
349 carbazole linker that we previously used for the preparation of  
350 metallotweezer 14, we prepared metallorectangle 17,<sup>28</sup> trigonal-  
351 prismatic metallocage 18,<sup>29</sup> and rhombohedral metallocy-  
352 clophane 19<sup>30</sup> (Scheme 14). Interestingly, the nanosized nature of  
353 the structures shown in Scheme 14, together with the presence  
354 of the two cofacial polycyclic-conjugated panels in 17 and 18,  
355 made these two latter assemblies very effective for the  
356 encapsulation of polycyclic aromatic hydrocarbons. In particu-  
357 lar, the hexagold prismatic cage 18 with the triphenylenetri-  
358 (NHC) ligand has a "slotlike" cavity with a volume of  $\sim 300$  Å<sup>3</sup>  
359 and a height of 7 Å. This cage shows a very large binding affinity  
360 for coronene, which makes it serve as an excellent coronene  
361 scavenger in CH<sub>2</sub>Cl<sub>2</sub>.<sup>29</sup> The perfect dimensional match between  
362 18 and coronene can be visualized in the structure shown in  
363 Figure 2. On the other hand, metallorectangle 17 shows very

high binding affinities for the encapsulation of planar PAHs in  
364 CH<sub>2</sub>Cl<sub>2</sub>. The binding constants were found to increase  
365 exponentially with the number of  $\pi$  electrons of the guest as a  
366 consequence of the enhancement of the host-guest face-to-face  
367 overlap, ranging from  $1.39 < \log K < 6.64$  for naphthalene  
368 through coronene.<sup>28</sup> These constants are among the highest  
369 found for a metal-containing receptor and compare well with  
370 those of the best organic-based cationic hosts.<sup>31</sup> The large  
371 binding affinities found for the case of 17 are due to the  
372 incorporation of the two cofacial pyrene panels separated by  
373 almost exactly 7 Å, thus providing an excellent dimensional  
374 match that makes that the encapsulation take place at a  
375 minimum energy cost due to the negligible structural distortions  
376 suffered by both the host and guest.<sup>28</sup> 377

A very interesting feature of metallorectangle 17 is that it is  
378 able to trap corannulene. As observed from the molecular  
379 structure of corannulene@17 (Figure 3b), the encapsulation of  
380 corannulene is accompanied by a significant compression of the  
381 bowl-shaped guest (the bowl depth of free corannulene is 0.87 Å,  
382 compared with 0.73 Å for the encapsulated one) and  
383 concomitant expansion of the host metallocage. The energy  
384 cost due to this mutual induced-fit arrangement and the lack of  
385 an effective  $\pi$ - $\pi$ -stacking interaction over the convex surface of  
386 the guest in corannulene@17 explain the reduced binding  
387 affinity shown for corannulene compared with its related planar  
388 20-electron PAH, perylene (compare the structures of  
389 perylene@17 and corannulene@17 in Figure 3).<sup>28</sup> 390

**Scheme 14. Gold-Based Metallosupramolecular Assemblies 17–19**





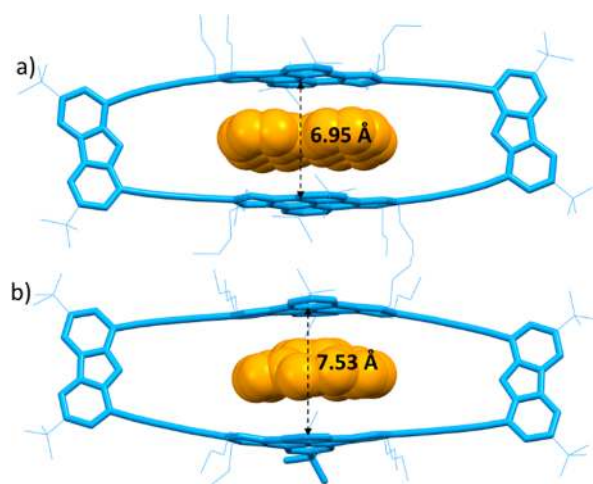


**Figure 3.** Molecular structures of (a) perylene@17 and (b) corannulene@17.

### 3.3. Metallorctangles, Metalloesquares, and Metalocages of Ni and Pd

391 of Ni and Pd

392 **3.3.1. Nickel.** Pyrenebis(NHC) ligand **C** (Scheme 2) used in  
 393 the preparation of tetragold(I) complex **17** turned out to be a  
 394 very useful synthon for the preparation of metallosupramolec-  
 395 ular structures with metals other than gold. By the use of this di-  
 396 NHC ligand, two nickel-cornered metallorctangles were  
 397 prepared whose dimensions were modulated by using either  
 398 pyrazine or 4,4'-bipyridine.<sup>32</sup> The metal-to-metal distance  
 399 established by the pyrenebis(imidazolyliene) ligands is ~13  
 400 Å, while the distances along the N-donor ligands are 7 and 11 Å  
 401 for pyrazine and bipyridine, respectively (Scheme 15). These  
 402 molecular rectangles were used for the encapsulation of PAHs.  
 403 Because of their dimensions, pyrazine-containing rectangle **20**  
 404 was able to host only one molecule of the polyaromatic guest,  
 405 while rectangle **21** containing bipyridine was capable of hosting  
 406 up to two guest molecules. Figure 4 shows the molecular  
 407 structure of (pyrene)<sub>2</sub>@**21**, where it can be observed that  
 408 effective  $\pi$ - $\pi$ -stacking interactions are established both between  
 409 the pyrene guest molecules and between the pyrene guests and  
 410 the pyrene moieties of the di-NHC ligands. The association  
 411 constants of the aromatic guests with both receptors were  
 412 determined in acetone-*d*<sub>6</sub>. The results showed that a good fit  
 413 between the size of the PAH and the binding constant could be

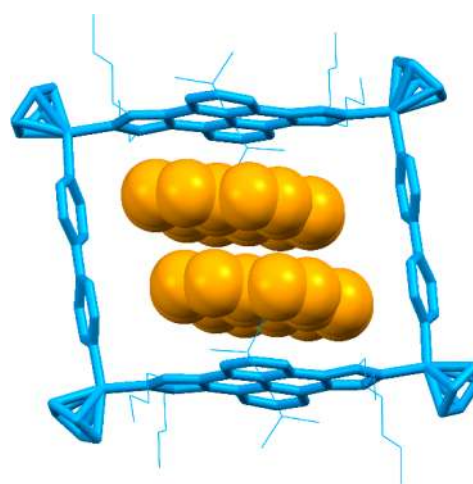
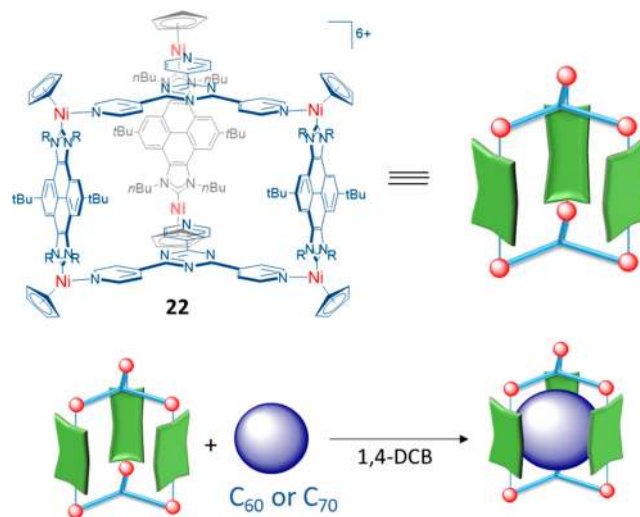


**Figure 4.** Molecular structure of (pyrene)<sub>2</sub>@**21**.

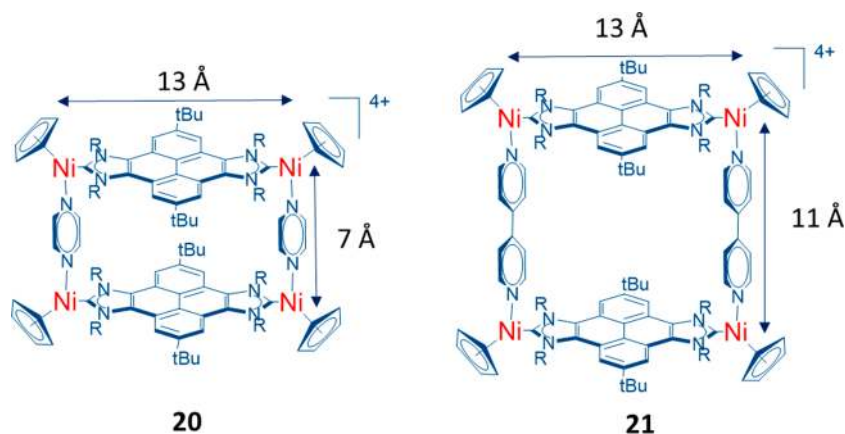
established by correlating the numbers of electrons of the guests 414  
 with their association constants.<sup>32</sup> 415

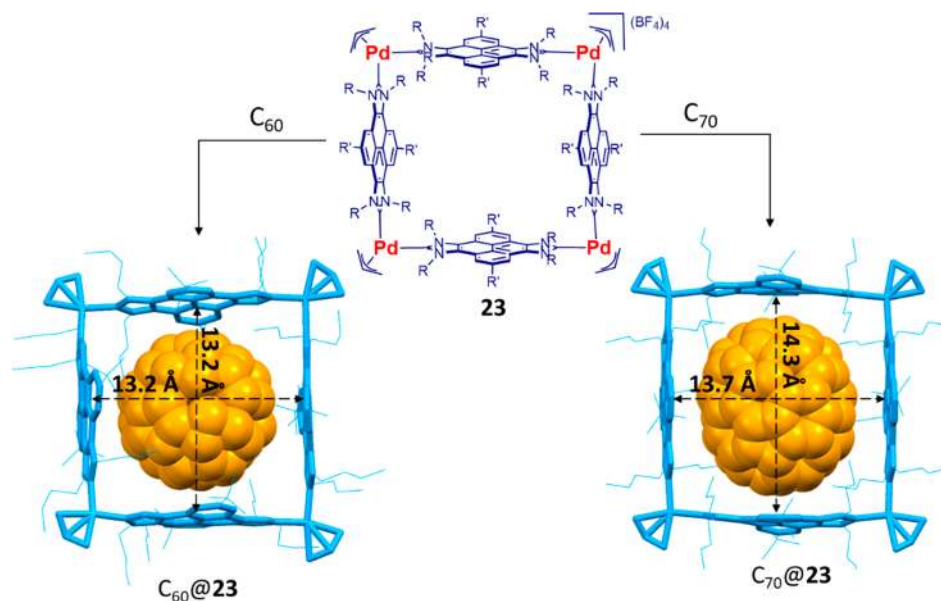
Using tripyridylpyrazine, we obtained trigonal prism **22** 416  
 (Scheme 16),<sup>33</sup> which was used for the encapsulation of 417 s16

### Scheme 16. Hexanickel Trigonal Prism **22** and Representation of Its Ability to Encapsulate C<sub>60</sub> and C<sub>70</sub>



### Scheme 15. Nickel-Cornered Metallorctangles **20** and **21**



Scheme 17. Palladium-Based Metallosquare **23** Used for the Encapsulation of  $C_{60}$  and  $C_{70}$ 

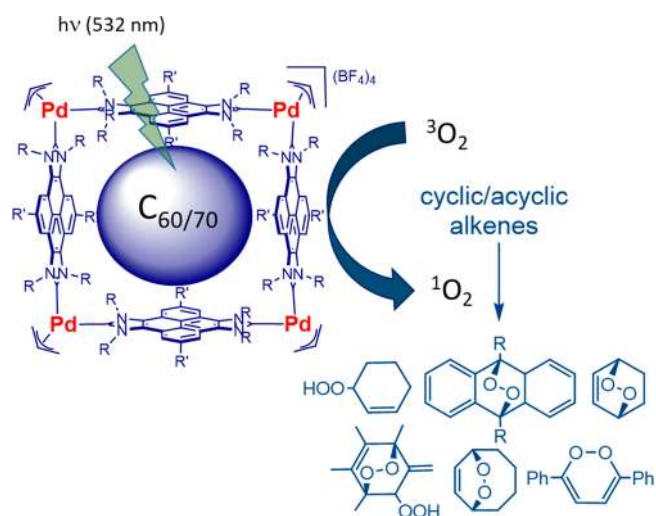
418 fullerenes  $C_{60}$  and  $C_{70}$ . The study of the binding affinities  
 419 showed that the cage exhibits highly selective complexation of  
 420  $C_{70}$  over  $C_{60}$ . The determination of the binding affinities at  
 421 different temperatures performed by  $^1\text{H}$  NMR spectroscopy in  
 422 1,2-dichlorobenzene allowed the determination of the thermo-  
 423 dynamic values associated with the binding process. For the  
 424 association of  $C_{60}$  and  $C_{70}$ , it was observed that the enthalpies  
 425 were low and positive as a consequence of the large solvation  
 426 enthalpies of both the free host and guests. For both fullerenes,  
 427 the association entropies were large and positive, thus indicating  
 428 that the process is entropically driven because of the desolvation  
 429 of both the host and guests. The higher entropy found for  $C_{70}$   
 430 with respect to  $C_{60}$  is a consequence of the larger surface area of  
 431 the former, which means that a larger number of solvent  
 432 molecules are bound to  $C_{70}$  relative to  $C_{60}$ .<sup>33</sup>

433 **3.3.2. Palladium.** The same pyrenebis(imidazolylidene)  
 434 ligand was used for the preparation of palladium-conjoined  
 435 molecular square **23** (Scheme 17).<sup>34</sup> The encapsulating  
 436 properties of this metallosquare are clearly determined by the  
 437 presence of the four pyrene panels, which endows the  
 438 compound a three-dimensional shape. This metallosquare was  
 439 used for the encapsulation of  $C_{60}$  and  $C_{70}$ . The metallosquare is  
 440 shape-adaptable in the sense that it can adjust to accommodate  
 441 the size of the encapsulated fullerene. The pyrene panels bend in  
 442 order to adapt their shapes to maximize the face-to-face overlap  
 443 with the convex surface of the fullerene (see Scheme 17), and  
 444 this also modifies the guest-available volume of the cavity. For  
 445 example, the distances between the center points of opposite  
 446 pyrene panels in  $C_{60}@23$  are significantly shorter than the  
 447 related distances in  $C_{70}@23$  (Scheme 17). The cage exhibits a  
 448 higher affinity for  $C_{70}$  over  $C_{60}$ , and the thermodynamic  
 449 parameters obtained from the determination of the association  
 450 constants at different temperatures show that the binding  
 451 process is entropically driven, and thus dominated by desolva-  
 452 tion rather than intrinsic interactions between the electron-  
 453 deficient fullerenes and the electron-rich faces of the pyrene  
 454 moieties of the metallosquare.<sup>34</sup>

455 An important feature of  $C_{60}@23$  and  $C_{70}@23$  is that both  
 456 host-guest complexes behaved as photochemically stable  
 457 singlet oxygen photosensitizers.<sup>35</sup> Both host-guest complexes

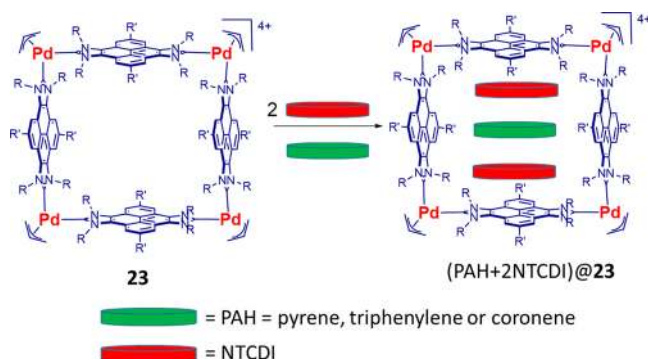
were used for the peroxidation of a series of cyclic and acyclic  
 458 alkenes at room temperature via visible-light-induced singlet  
 459 oxygen generation. By measuring the phosphorescence emission  
 460 spectra of singlet oxygen generated by the two complexes upon  
 461 irradiation with visible light,  $^1\text{O}_2$  quantum yields of  $\Phi_{\Delta} = 0.23$   
 462 and 0.41 were obtained for  $C_{60}@23$  and  $C_{70}@23$ , respectively.  
 463 This explains why the activity shown by  $C_{70}@23$  in the  
 464 photocatalytic peroxidations was higher than that shown by  
 465  $C_{60}@23$ .<sup>35</sup> The photosensitizing properties of these two  
 466 fullerene-containing cages is explained by the excellent spin-  
 467 converting properties of fullerenes, which make them excep-  
 468 tional agents for singlet oxygen production (Scheme 18). These  
 469 s18 results are important because they underline the possibility that  
 470 other fullerene-containing supramolecular systems have the  
 471 potential to be used for similar catalytic reactions.  
 472

Another interesting feature of metallocage **23** is that it displays  
 473 a metal-to-metal distance of 13 Å, which is approximately 4  
 474 times the distance for an effective  $\pi$ - $\pi$ -stacking interaction and  
 475

Scheme 18.  $C_{60}@23$  and  $C_{70}@23$  Used as Photocatalysts for Peroxidation of Alkenes

476 therefore optimum for encapsulating up to three polyaromatic  
477 guests. In fact, the complex is able to encapsulate one molecule  
478 of an electron-rich polycyclic aromatic hydrocarbon (pyrene,  
479 triphenylene, or coronene) and two molecules of electron-  
480 deficient *N,N'*-dimethyl-naphthalenetetracarboxydiimide  
481 (NTCDI).<sup>36</sup> This forms quintuple  $\pi$  stacks ordered in donor–  
482 acceptor–donor–acceptor–donor (D–A–D–A–D) arrays  
483 (Scheme 19), with the electron-rich pyrene fragments of the

**Scheme 19. Quintuple D–A–D–A–D  $\pi$  Stack Formed by Heteroguest Encapsulation in 23**



484 di-NHC ligand of the cage as bookend donors. The fact that 23  
485 is able to trap large  $\pi$ -conjugated heteroguests to form quintuple  
486  $\pi$  stacks is interesting because most systems previously used for  
487 the encapsulation of heteroguests are based on “closed” trigonal-  
488 prismatic architectures, while ours is an “open” square structure.

#### 4. CONCLUSIONS AND OUTLOOK

489 In this Account, we have described our most recent work on the  
490 preparation of NHC-based metallosupramolecular assemblies  
491 and their host–guest chemistry properties. We have tried to  
492 emphasize that NHC ligands bearing planar polyaromatic  
493 connectors offer a powerful tool for building hollow organo-  
494 metallic supramolecular receptors, including metallotweezers,  
495 metallosquares, metallorectangles, and trigonal-prismatic metal-  
496 locages. The use of these systems as hosts for organic or  
497 inorganic guests is directed by the intentional combination of  
498 supramolecular interactions, including  $\pi$ – $\pi$ -stacking, hydrogen-  
499 bonding, and metallophilic interactions.

500 We once used the term “smart ligands” to refer to NHCs,  
501 meaning that NHC chemistry has rapidly adapted to new times  
502 and needs for novel reactivities, especially in the design of more  
503 effective homogeneous catalysts.<sup>37</sup> The results shown in this  
504 Account illustrate how NHC ligands have also adapted to the  
505 field of supramolecular chemistry, and therefore, NHC ligands  
506 can be also considered smart in this field of chemistry. Probably  
507 one of the advantages that needs to be highlighted here is that  
508 now there is an extensive library of NHC ligands decorated with  
509 rigid polyaromatic moieties that can provide clear advantages  
510 over other traditional Werner-type ligands used in metal-  
511 losupramolecular chemistry, for which the incorporation of  
512 these planar polyconjugated fragments is much more difficult to  
513 achieve. Another important feature that needs to be considered  
514 is that most of the NHC-based supramolecular assemblies  
515 described here are remarkably stable and can remain intact in  
516 solution for days without signs of decomposition. This obviously  
517 widens their potential use for practical applications. In this  
518 regard, we expect that further effort will be applied in several  
519 directions, for example toward the exploitation of the singlet

oxygen generation properties of fullerene-containing supra-  
molecular assemblies, not only from the photocatalytic point of  
view but also as potential agents for clinical photodynamic  
therapy (PDT). In addition, on the basis of the biomedical  
activity shown by other Au- and Ag-containing NHC-based  
supramolecular assemblies,<sup>16</sup> studies can be directed to prospect  
the biological applications of this type of system, possibly by  
including in the NHC scaffolds further functionalities that can  
target biological units (i.e., peptides), which to date has been  
mostly explored with small molecules.<sup>38</sup>

Efforts can also be directed toward the reversible  
encapsulation of homogeneous catalysts, which may be released  
on demand by the addition of, for example, an additive guest  
with a higher binding affinity with the receptor. Finally, the  
possibility that supramolecular organometallic complexes can  
form stable discrete multiple stacks may have important  
implications for the design of nanoscale electronic devices  
because enabling discrete  $\pi$  stacks can facilitate the study of  
charge transport at the molecular level. In summary, we hope  
that the findings described in this Account will help advance in  
the field of supramolecular organometallic host–guest chem-  
istry.

#### ■ ASSOCIATED CONTENT

##### Supporting Information

The Supporting Information is available free of charge at  
<https://pubs.acs.org/doi/10.1021/acs.accounts.0c00312>.

Crystallographic data for 3-perylenylmethanol@14 (CIF)

#### ■ AUTHOR INFORMATION

##### Corresponding Author

**Eduardo Peris** – Institute of Advanced Materials (INAM), Centro  
de Innovación en Química Avanzada (ORFEO–CINQA),  
Universitat Jaume I, E-12071 Castellón, Spain; [orcid.org/0000-0001-9022-2392](https://orcid.org/0000-0001-9022-2392); Email: [eperis@uji.es](mailto:eperis@uji.es)

##### Authors

**Susana Ibáñez** – Institute of Advanced Materials (INAM), Centro  
de Innovación en Química Avanzada (ORFEO–CINQA),  
Universitat Jaume I, E-12071 Castellón, Spain

**Macarena Poyatos** – Institute of Advanced Materials (INAM),  
Centro de Innovación en Química Avanzada  
(ORFEO–CINQA), Universitat Jaume I, E-12071 Castellón,  
Spain; [orcid.org/0000-0003-2000-5231](https://orcid.org/0000-0003-2000-5231)

Complete contact information is available at:  
<https://pubs.acs.org/10.1021/acs.accounts.0c00312>

##### Author Contributions

The manuscript was written through contributions of all  
authors. All of the authors approved the final version of the  
manuscript.

##### Notes

The authors declare no competing financial interest.

##### Biographies

**Susana Ibáñez** graduated in Chemistry in 2001 at the University of  
Zaragoza. She received her Ph.D. degree with European Doctorate in  
2007 at the University of Zaragoza. She then moved to Bari (Italy) as a  
postdoctoral fellow under the supervision of Prof. Piero Mastrorilli. In  
2009 she joined Prof. Bernhard Lippert at Technische Universität



575 Dortmund, where she stayed for 2 years. In 2014 she joined Prof.  
576 Eduardo Peris' group at Universitat Jaume I as an associate researcher.

577 **Macarena Poyatos** graduated in Chemistry at Universitat Jaume I  
578 (Castellón, Spain). She received her Ph.D. degree in 2005 at Universitat  
579 Jaume I under the supervision of Prof. Eduardo Peris. She then moved  
580 to Strasbourg, where she joined the group supervised by Prof. Lutz H.  
581 Gade and Dr. Stéphane Bellemin-Laponnaz. In 2006 she joined Prof.  
582 Robert H. Crabtree's group at Yale University, where she stayed for 2  
583 years. In 2008 she returned to Universitat Jaume I, where she currently  
584 holds a position as an associate professor.

585 **Eduardo Peris** received his Ph.D. degree in Chemistry in 1991 at the  
586 Universidad de Valencia. In 1994 he joined Robert Crabtree's group at  
587 Yale University, where he stayed for 2 years. In October 1995 he moved  
588 to Universitat Jaume I, where he currently holds a position as a full  
589 professor. The current interest of his group is the development of  
590 organometallic-based supramolecular systems for the development of  
591 host-guest receptors and improved catalysts.

## 592 ■ ACKNOWLEDGMENTS

593 We gratefully acknowledge financial support from the Ministerio  
594 de Ciencia e Innovación (PGC2018-093382-B-I00) and  
595 Universitat Jaume I (UJI-B2017-07 and UJI-A2017-02). E.P.  
596 thanks the Alexander von Humboldt Foundation for a  
597 Humboldt Research Award.

## 598 ■ REFERENCES

599 (1) (a) Chakrabarty, R.; Mukherjee, P. S.; Stang, P. J. Supramolecular  
600 Coordination: Self-Assembly of Finite Two- and Three-Dimensional  
601 Ensembles. *Chem. Rev.* **2011**, *111*, 6810–6918. (b) Smulders, M. M. J.;  
602 Riddell, I. A.; Browne, C.; Nitschke, J. R. Building on architectural  
603 principles for three-dimensional metallosupramolecular construction.  
604 *Chem. Soc. Rev.* **2013**, *42*, 1728–1754. (c) Constable, E. C. Expanded  
605 ligands - An assembly principle for supramolecular chemistry. *Coord.*  
606 *Chem. Rev.* **2008**, *252*, 842–855. (d) Wang, W.; Wang, Y. X.; Yang, H.  
607 B. Supramolecular transformations within discrete coordination-driven  
608 supramolecular architectures. *Chem. Soc. Rev.* **2016**, *45*, 2656–2693.

609 (2) (a) Cook, T. R.; Stang, P. J. Recent Developments in the  
610 Preparation and Chemistry of Metallacycles and Metallacages via  
611 Coordination. *Chem. Rev.* **2015**, *115*, 7001–7045. (b) Castilla, A. M.;  
612 Ramsay, W. J.; Nitschke, J. R. Stereochemistry in Subcomponent Self-  
613 Assembly. *Acc. Chem. Res.* **2014**, *47*, 2063–2073. (c) McConnell, A. J.;  
614 Wood, C. S.; Neelakandan, P. P.; Nitschke, J. R. Stimuli-Responsive  
615 Metal-Ligand Assemblies. *Chem. Rev.* **2015**, *115*, 7729–7793.  
616 (d) Fujita, M. Metal-directed self-assembly of two- and three-  
617 dimensional synthetic receptors. *Chem. Soc. Rev.* **1998**, *27*, 417–425.

618 (3) (a) Otte, M. Size-Selective Molecular Flasks. *ACS Catal.* **2016**, *6*,  
619 6491–6510. (b) Yoshizawa, M.; Klosterman, J. K.; Fujita, M.  
620 Functional Molecular Flasks: New Properties and Reactions within  
621 Discrete, Self-Assembled Hosts. *Angew. Chem., Int. Ed.* **2009**, *48*, 3418–  
622 3438.

623 (4) Poyatos, M.; Mata, J. A.; Peris, E. Complexes with poly(N-  
624 heterocyclic carbene) ligands: structural features and catalytic  
625 applications. *Chem. Rev.* **2009**, *109*, 3677–3707.

626 (5) (a) Gan, M. M.; Liu, J. Q.; Zhang, L.; Wang, Y. Y.; Hahn, F. E.;  
627 Han, Y. F. Preparation and Post-Assembly Modification of Metal-  
628 losupramolecular Assemblies from Poly(N-Heterocyclic Carbene)  
629 Ligands. *Chem. Rev.* **2018**, *118*, 9587–9641. (b) Sinha, N.; Hahn, F.  
630 E. Metallosupramolecular Architectures Obtained from Poly-N-  
631 heterocyclic Carbene Ligands. *Acc. Chem. Res.* **2017**, *50*, 2167–2184.  
632 (c) Pöthig, A.; Casini, A. Recent Developments of Supramolecular  
633 Metal-Based Structures for Applications in Cancer Therapy and  
634 Imaging. *Theranostics* **2019**, *9*, 3150–3169.

635 (6) (a) Conrady, F. M.; Fröhlich, R.; Schulte to Brinke, C.; Pape, T.;  
636 Hahn, F. E. Stepwise Formation of a Molecular Square with Bridging  
637 NH, O-Substituted Dicarbene Building Blocks. *J. Am. Chem. Soc.* **2011**,

133, 11496–11499. (b) Schmidtendorf, M.; Pape, T.; Hahn, F. E. 638  
Stepwise Preparation of a Molecular Square from NR, NR-, O- 639  
Substituted Dicarbene Building Blocks. *Angew. Chem., Int. Ed.* **2012**, *51*, 640  
2195–2198. (c) Mejuto, C.; Guisado-Barrios, G.; Gusev, D.; Peris, E. 641  
First homoleptic MIC and heteroleptic NHC-MIC coordination cages 642  
from 1,3,5-triphenylbenzene-bridged tris-MIC and tris-NHC ligands. 643  
*Chem. Commun.* **2015**, *51*, 13914–13917. 644

(7) (a) Radloff, C.; Gong, H. Y.; Schulte to Brinke, C.; Pape, T.; 645  
Lynch, V. M.; Sessler, J. L.; Hahn, F. E. Metal-Dependent Coordination 646  
Modes Displayed by Macrocyclic Polycarbene Ligands. *Chem. - Eur. J.* 647  
**2010**, *16*, 13077–13081. (b) Rit, A.; Pape, T.; Hahn, F. E. Self- 648  
Assembly of Molecular Cylinders from Polycarbene Ligands and Ag<sup>I</sup> or 649  
Au<sup>I</sup>. *J. Am. Chem. Soc.* **2010**, *132*, 4572–4573. (c) Rit, A.; Pape, T.; 650  
Hepp, A.; Hahn, F. E. Supramolecular Structures from Polycarbene 651  
Ligands and Transition Metal Ions. *Organometallics* **2011**, *30*, 334– 652  
347. (d) Wang, D. H.; Zhang, B. G.; He, C.; Wu, P. Y.; Duan, C. Y. A 653  
new chiral N-heterocyclic carbene silver(I) cylinder: synthesis, crystal 654  
structure and catalytic properties. *Chem. Commun.* **2010**, *46*, 4728– 655  
4730. (e) Segarra, C.; Guisado-Barrios, G.; Hahn, F. E.; Peris, E. 656  
Hexanuclear cylinder-shaped assemblies of silver and gold from 657  
benzene-hexa-N-heterocyclic carbenes. *Organometallics* **2014**, *33*, 658  
5077–5080. (f) Sinha, N.; Roelfes, F.; Hepp, A.; Mejuto, C.; Peris, 659  
E.; Hahn, F. E. Synthesis of Nanometer-Sized Cylinder-Like Structures 660  
from a 1,3,5-Triphenylbenzene-Bridged Tris-NHC Ligand and Ag<sup>I</sup>, 661  
Au<sup>I</sup>, and Cu<sup>I</sup>. *Organometallics* **2014**, *33*, 6898–6904. (g) Sinha, N.; 662  
Stegemann, L.; Tan, T. T. Y.; Doltsinis, N. L.; Strassert, C. A.; Hahn, F. 663  
E. Turn-On Fluorescence in Tetra-NHC Ligands by Rigidification 664  
through Metal Complexation: An Alternative to Aggregation-Induced 665  
Emission. *Angew. Chem., Int. Ed.* **2017**, *56*, 2785–2789. (h) Li, Y.; An, 666  
Y. Y.; Fan, J. Z.; Liu, X. X.; Li, X.; Hahn, F. E.; Wang, Y. Y.; Han, Y. F. 667  
Strategy for the Construction of Diverse Poly-NHC-Derived 668  
Assemblies and Their Photoinduced Transformations. *Angew. Chem.,* 669  
*Int. Ed.* **2020**, *59*, 10073–10080. 670

(8) (a) Mas-Marza, E.; Mata, J. A.; Peris, E. Triazole-diylienes: A 671  
versatile class of ligands for the preparation of discrete molecules of 672  
homo- and hetero-binuclear complexes for improved catalytic 673  
applications. *Angew. Chem., Int. Ed.* **2007**, *46*, 3729–3731. (b) Prades, 674  
A.; Peris, E.; Alcarazo, M. Pyracenebis(imidazolylidene): a new Janus- 675  
type biscarbene and its coordination to rhodium and iridium. 676  
*Organometallics* **2012**, *31*, 4623–4626. (c) Gonell, S.; Poyatos, M.; 677  
Peris, E. Pyrene-Based Bisazolium Salts: From Luminescence Proper- 678  
ties to Janus-Type Bis-N-Heterocyclic Carbenes. *Chem. - Eur. J.* **2014**, 679  
*20*, 9716–9724. (d) Gonell, S.; Poyatos, M.; Peris, E. Triphenylene- 680  
Based Tris(N-Heterocyclic Carbene) Ligand: Unexpected Catalytic 681  
Benefits. *Angew. Chem., Int. Ed.* **2013**, *52*, 7009–7013. (e) Valdes, H.; 682  
Poyatos, M.; Peris, E. A Nanosized Janus Bis-N-heterocyclic Carbene 683  
Ligand Based on a Quinoxalinophenanthrophenazine Core, and Its 684  
Coordination to Iridium. *Organometallics* **2015**, *34*, 1725–1729. 685  
(f) Ibáñez, S.; Poyatos, M.; Peris, E. A D<sub>3h</sub>-symmetry hexaazatriphene- 686  
nylene-tris-N-heterocyclic carbene ligand and its coordination to 687  
iridium and gold: preliminary catalytic studies. *Chem. Commun.* **2017**, 688  
*53*, 3733–3736. (g) Valdes, H.; Poyatos, M.; Peris, E. A Pyrene-Based 689  
N-Heterocyclic Carbene: Study of Its Coordination Chemistry and 690  
Stereoelectronic Properties. *Organometallics* **2014**, *33*, 394–401. 691

(9) (a) Boydston, A. J.; Bielawski, C. W. Bis(imidazolylidene)s as 692  
modular building blocks for monomeric and macromolecular organo- 693  
metallic materials. *Dalton Trans.* **2006**, 4073–4077. (b) Boydston, A. J.; 694  
Williams, K. A.; Bielawski, C. W. A modular approach to main-chain 695  
organometallic polymers. *J. Am. Chem. Soc.* **2005**, *127*, 12496–12497. 696

(10) Segarra, C.; Linke, J.; Mas-Marza, E.; Kuck, D.; Peris, E. A C<sub>3v</sub>- 697  
symmetrical tribenzotriquinacene-based threefold N-heterocyclic 698  
carbene. Coordination to rhodium(I) and stereoelectronic properties. 699  
*Chem. Commun.* **2013**, *49*, 10572–10574. 700

(11) Radloff, C.; Weigand, J. J.; Hahn, F. E. A tetranuclear molecular 701  
rectangle from four gold(I) atoms linked by dicarbene and diphosphine 702  
ligands. *Dalton Trans.* **2009**, 9392–9394. 703

(12) (a) Schmidtendorf, M.; Schulte to Brinke, C.; Hahn, F. E. 704  
Benzodicarbene-bridged dinuclear complexes as building blocks for 705  
metallosupramolecular architectures. *J. Organomet. Chem.* **2014**, *751*, 706

- 707 620–627. (b) Sinha, A.; Roelfes, F.; Hepp, A.; Hahn, E. F. Single-Step  
708 Synthesis of Organometallic Molecular Squares from NR, NR', NR'',  
709 NR'''-Substituted Benzobiscarbenes. *Chem. - Eur. J.* **2017**, *23*, 5939–  
710 5942.
- 711 (13) Schmidtdorf, M.; Pape, T.; Hahn, F. E. Molecular rectangles  
712 from platinum(II) and bridging dicarbene, diisocyanide and 4,4'-  
713 bipyridine ligands. *Dalton Trans.* **2013**, *42*, 16128–16141.
- 714 (14) Radloff, C.; Hahn, F. E.; Pape, T.; Fröhlich, R. Supramolecular  
715 structures from mono and dimetalated biscarbene ligands. *Dalton*  
716 *Trans.* **2009**, 7215–7222.
- 717 (15) (a) Altmann, P. J.; Pöthig, A. Pillarplexes: A Metal–Organic  
718 Class of Supramolecular Hosts. *J. Am. Chem. Soc.* **2016**, *138*, 13171–  
719 13174. (b) Altmann, P. J.; Pöthig, A. A pH-Dependent, Mechanically  
720 Interlocked Switch: Organometallic [2]Rotaxane vs. Organic [3]-  
721 Rotaxane. *Angew. Chem., Int. Ed.* **2017**, *56*, 15733–15736.
- 722 (16) Pöthig, A.; Ahmed, S.; Winther-Larsen, H. C.; Guan, S.; Altmann,  
723 P. J.; Kudermann, J.; Santos Andresen, A. M.; Gjøen, T.; Høgmoen  
724 Åstrand, O. A. Antimicrobial Activity and Cytotoxicity of Ag(I) and  
725 Au(I) Pillarplexes. *Front. Chem.* **2018**, *6*, 584.
- 726 (17) Peris, E. Polyaromatic N-heterocyclic carbene ligands and pi-  
727 stacking. Catalytic consequences. *Chem. Commun.* **2016**, *52*, 5777–  
728 5787.
- 729 (18) (a) Hardouin-Lerouge, M.; Hudhomme, P.; Salle, M. Molecular  
730 clips and tweezers hosting neutral guests. *Chem. Soc. Rev.* **2011**, *40*, 30–  
731 43. (b) Klarner, F. G.; Kahlert, B. Molecular tweezers and clips as  
732 synthetic receptors. Molecular recognition and dynamics in receptor-  
733 substrate complexes. *Acc. Chem. Res.* **2003**, *36*, 919–932. (c) Klarner, F.  
734 G.; Schrader, T. Aromatic Interactions by Molecular Tweezers and  
735 Clips in Chemical and Biological Systems. *Acc. Chem. Res.* **2013**, *46*,  
736 967–978. (d) Leblond, J.; Petitjean, A. Molecular Tweezers: Concepts  
737 and Applications. *ChemPhysChem* **2011**, *12*, 1043–1051.
- 738 (19) (a) Alvarez, C. M.; Garcia-Escudero, L. A.; Garcia-Rodriguez, R.;  
739 Martin-Alvarez, J. M.; Miguel, D.; Rayon, V. M. Enhanced association  
740 for C-70 over C-60 with a metal complex with corannulene derivate  
741 ligands. *Dalton Trans.* **2014**, *43*, 15693–15696. (b) Tanaka, Y.; Wong,  
742 K. M. C.; Yam, V. W. W. Platinum-Based Phosphorescent Double-  
743 Decker Tweezers: A Strategy for Extended Heterologous Metal-Metal  
744 Interactions. *Angew. Chem., Int. Ed.* **2013**, *52*, 14117–14120.
- 745 (c) Tanaka, Y.; Wong, K. M. C.; Yam, V. W. W. Host-Guest  
746 Interactions of Phosphorescent Molecular Tweezers Based on an  
747 Alkynylplatinum(II) Terpyridine System with Polyaromatic Hydro-  
748 carbons. *Chem. - Eur. J.* **2013**, *19*, 390–399. (d) Fu, T. F.; Han, Y. F.;  
749 Ao, L.; Wang, F. Bis alkynylplatinum(II) Terpyridine Molecular  
750 Tweezer/Guest Recognition Enhanced by Intermolecular Hydrogen  
751 Bonds: Phototriggered Complexation via the “Caging” Strategy.  
752 *Organometallics* **2016**, *35*, 2850–2853. (e) Doistau, B.; Rossi-  
753 Gendron, C.; Tron, A.; McClenaghan, N. D.; Chamoreau, L. M.;  
754 Hasenknopf, B.; Vives, G. Switchable platinum-based tweezers with Pt-  
755 Pt bonding and selective luminescence quenching. *Dalton Trans.* **2015**,  
756 *44*, 8543–8551. (f) Chan, A. K. W.; Yam, V. W. W. Precise Modulation  
757 of Molecular Building Blocks from Tweezers to Rectangles for  
758 Recognition and Stimuli-Responsive Processes. *Acc. Chem. Res.* **2018**,  
759 *51*, 3041–3051. (g) Crowley, J. D.; Bosnich, B. Molecular recognition:  
760 Use of metal-containing molecular clefts for supramolecular self-  
761 assembly and host-guest formation. *Eur. J. Inorg. Chem.* **2005**, *2005*,  
762 2015–2025.
- 763 (20) Nuevo, D.; Gonell, S.; Poyatos, M.; Peris, E. Platinum-Based  
764 Organometallic Folders for the Recognition of Electron-Deficient  
765 Aromatic Substrates. *Chem. - Eur. J.* **2017**, *23*, 7272–7277.
- 766 (21) Ibáñez, S.; Poyatos, M.; Peris, E. Cation-Driven Self-Assembly of  
767 a Gold(I)-Based Metallo-Tweezer. *Angew. Chem., Int. Ed.* **2017**, *56*,  
768 9786–9790.
- 769 (22) Ibáñez, S.; Peris, E. Chemically Tunable Formation of Different  
770 Discrete, Oligomeric, and Polymeric Self-Assembled Structures from  
771 Digold Metallotweezers. *Chem. - Eur. J.* **2018**, *24*, 8424–8431.
- 772 (23) Ibáñez, S.; Peris, E. A Matter of Fidelity: Self-Sorting Behavior of  
773 Di-Gold Metallotweezers. *Chem. - Eur. J.* **2019**, *25*, 8254–8258.
- 774 (24) Wang, Y. S.; Feng, T.; Wang, Y. Y.; Hahn, F. E.; Han, Y. F. Homo-  
775 and Heteroligand Poly-NHC Metal Assemblies: Synthesis by  
Narcissistic and Social Self-Sorting. *Angew. Chem., Int. Ed.* **2018**, *57*,  
15767–15771.
- (25) Ibáñez, S.; Poyatos, M.; Peris, E. The Complex Coordination  
778 Landscape of a Digold(I) U-Shaped Metalloligand. *Angew. Chem., Int.*  
779 *Ed.* **2018**, *57*, 16816–16820.
- (26) Biz, C.; Ibáñez, S.; Poyatos, M.; Gusev, D.; Peris, E. Gold(I)  
781 Metallo-Tweezers for the Recognition of Functionalized Polycyclic  
782 Aromatic Hydrocarbons by Combined pi-pi Stacking and H-Bonding.  
783 *Chem. - Eur. J.* **2017**, *23*, 14439–14444.
- (27) Nuevo, D.; Poyatos, M.; Peris, E. A Dinuclear Au(I) Complex  
785 with a Pyrene-di-N-heterocyclic Carbene Linker: Supramolecular and  
786 Catalytic Studies. *Organometallics* **2018**, *37*, 3407–3411.
- (28) Ibáñez, S.; Peris, E. Dimensional Matching versus Induced-Fit  
788 Distortions: Binding Affinities of Planar and Curved Polyaromatic  
789 Hydrocarbons with a Tetragold Metallorectangle. *Angew. Chem., Int.*  
790 *Ed.* **2020**, *59*, 6860–6865.
- (29) Ibáñez, S.; Peris, E. A Rigid Trigonal-Prismatic Hexagold  
792 Metallocage That Behaves as a Coronene Trap. *Angew. Chem., Int. Ed.*  
793 **2019**, *58*, 6693–6697.
- (30) Gutierrez-Blanco, A.; Ibáñez, S.; Hahn, F. E.; Poyatos, M.; Peris,  
795 E. A Twisted Tetragold Cyclophane from a Fused Bis-Imidazolindiy-  
796 lidene. *Organometallics* **2019**, *38*, 4565–4569.
- (31) (a) Dale, E. J.; Vermeulen, N. A.; Thomas, A. A.; Barnes, J. C.;  
798 Juricek, M.; Blackburn, A. K.; Strutt, N. L.; Sarjeant, A. A.; Stern, C. L.;  
799 Denmark, S. E.; Stoddart, J. F. ExCage. *J. Am. Chem. Soc.* **2014**, *136*,  
800 10669–10682. (b) Barnes, J. C.; Juricek, M.; Strutt, N. L.; Frasconi, M.;  
801 Sampath, S.; Giesener, M. A.; McGrier, P. L.; Bruns, C. J.; Stern, C. L.;  
802 Sarjeant, A. A.; Stoddart, J. F. ExBox: A Polycyclic Aromatic  
803 Hydrocarbon Scavenger. *J. Am. Chem. Soc.* **2013**, *135*, 183–192.
- (32) Martinez-Agramunt, V.; Ruiz-Botella, S.; Peris, E. Nickel-  
805 Cornered Molecular Rectangles as Polycyclic Aromatic Hydrocarbon  
806 Receptors. *Chem. - Eur. J.* **2017**, *23*, 6675–6681.
- (33) Martinez-Agramunt, V.; Gusev, D. G.; Peris, E. A Shape-  
808 Adaptable Organometallic Supramolecular Coordination Cage for the  
809 Encapsulation of Fullerenes. *Chem. - Eur. J.* **2018**, *24*, 14802–14807.
- (34) Martinez-Agramunt, V.; Eder, T.; Darmandeh, H.; Guisado-  
811 Barrios, G.; Peris, E. A Size-Flexible Organometallic Box for the  
812 Encapsulation of Fullerenes. *Angew. Chem., Int. Ed.* **2019**, *58*, 5682–  
813 5686.
- (35) Martinez-Agramunt, V.; Peris, E. Photocatalytic Properties of a  
815 Palladium Metallosquare with Encapsulated Fullerenes via Singlet  
816 Oxygen Generation. *Inorg. Chem.* **2019**, *58*, 11836–11842.
- (36) Martinez-Agramunt, V.; Peris, E. A palladium-hinged organo-  
818 metallic square with a perfect-sized cavity for the encapsulation of three  
819 heteroguests. *Chem. Commun.* **2019**, *55*, 14972–14975.
- (37) Peris, E. Smart N-heterocyclic carbene ligands in catalysis. *Chem.*  
821 *Rev.* **2018**, *118*, 9988–10031.
- (38) Meier-Menches, S. M.; Casini, A. Design Strategies and  
823 Medicinal Applications of Metal–Peptidic Bioconjugates. *Bioconjugate*  
824 *Chem.* **2020**, *31*, 1279–1288.